



Aalborg Universitet

AALBORG UNIVERSITY
DENMARK

Controlling a Conventional LS-pump based on Electrically Measured LS-pressure

Pedersen, Henrik Clemmensen; Andersen, Torben Ole; Hansen, Michael Rygaard

Published in:
Proceeding of the Fluid Power and Motion Control (FPMC'08)

Publication date:
2008

Document Version
Publisher's PDF, also known as Version of record

[Link to publication from Aalborg University](#)

Citation for published version (APA):
Pedersen, H. C., Andersen, T. O., & Hansen, M. R. (2008). Controlling a Conventional LS-pump based on Electrically Measured LS-pressure. In *Proceeding of the Fluid Power and Motion Control (FPMC'08)* Bath University, The Centre for Power Transmission and Motion Control.

General rights

Copyright and moral rights for the publications made accessible in the public portal are retained by the authors and/or other copyright owners and it is a condition of accessing publications that users recognise and abide by the legal requirements associated with these rights.

- ? Users may download and print one copy of any publication from the public portal for the purpose of private study or research.
- ? You may not further distribute the material or use it for any profit-making activity or commercial gain
- ? You may freely distribute the URL identifying the publication in the public portal ?

Take down policy

If you believe that this document breaches copyright please contact us at vbn@aub.aau.dk providing details, and we will remove access to the work immediately and investigate your claim.

Controlling a Conventional LS-pump based on Electrically Measured LS-pressure

Torben O. Andersen
Professor, Ph.D.
Energy Technology
Aalborg University
DK-9220 Aalborg East
+45 9940 9269
toa@iet.aau.dk

Henrik C. Pedersen
Ass. Professor, Ph.D.
Energy Technology
Aalborg University
DK-9220 Aalborg East
+45 9940 9275
hcp@iet.aau.dk

Michael R. Hansen
Asc. Professor, Ph.D.
Mechanical Engineering
Aalborg University
DK-9220 Aalborg East
+45 9940 9321
mrh@ime.aau.dk

ABSTRACT

As a result of the increasing use of sensors in mobile hydraulic equipment, the need for hydraulic pilot lines is decreasing, being replaced by electrical wiring and electrically controllable components. For controlling some of the existing hydraulic components there are, however, still a need for being able to generate a hydraulic pilot pressure. In this paper controlling a hydraulic variable pump is considered. The LS-pressure is measured electrically and the hydraulic pilot pressure is generated using a small spool valve. From a control point of view there are two approaches for controlling this system, by either generating a copy of the LS-pressure, the LS-pressure being the output, or letting the output be the pump pressure. The focus of the current paper is on the controller design based on the first approach. Specifically a controlled leakage flow is used to avoid the need for a switching control structure.

1 INTRODUCTION

The development of hydraulic systems shows a clear tendency towards electrically controlled components, as pointed out by e.g. [1]. This also means that the need for hydraulic pilot lines is decreasing, as load pressures are starting to be measured and distributed electronically instead of hydraulically. However, in the transition phase between traditionally hydraulically controlled components and fully electrically controlled systems, some components may still need a hydraulic LS pressure to operate, and there is a need for being able to generate this hydraulic LS pressure based on an electrical reference. One such example is e.g. where a hydraulic LS-pump is connected to an otherwise electronically controlled system, where there is no hydraulic LS-pressure available. This problem is the objective of the current paper, where focus is on generating a hydraulic LS-pressure for a conventional variable displacement pump.

To the knowledge of the authors, no other such solution has been made; although the problem has some resemblance to controlling the pump pressure in an electronic load sensing

system, which has been the subject of several studies, see e.g. [2, 3, 4, 5, 6, 7]. Common for these studies are that they have used a sufficiently fast servo valve/proportional valve directly controlling the flow to the displacement piston of the pump. Hence removing the original hydro-mechanical LS-regulator in the pump and in effect replacing the dynamics of the hydro-mechanical LS-regulator and pilot line. The idea of using an artificially generated LS-pressure has also indirectly been presented by [8] as part of a pump regulator, where the LS-pressure was generated based on the pump pressure using a series connection consisting of a fixed orifice and electrically controlled relief valve, hereby obtaining the effect of a pressure divider. Apart from the idea of generating the LS-pressure based on the pump pressure, the two solutions do however pose different problems, not only due to different topologies and control problems, but also as the presented solution is intended to be mounted a distance away from the pump and should be applicable in combination with a large variation of pumps.

The paper first presents the considered system and an experimentally verified model. For stability analysis a linearized model is derived and sensitivity of the system to varying operating conditions discussed. Based on the results of this analysis the controller design is presented and robustness evaluated. Finally, experimental results are presented, and the performance of the electro-hydraulic pressure regulator is compared to that of the hydraulic reference system.

2 SYSTEM MODELLING

The system considered consists of the pump, spool valve, hoses and the load system, as shown in figure 1. From the figure it is seen that the set-up may also be used as a classical LS-system (parallel circuit), making it possible to test the two systems individually.

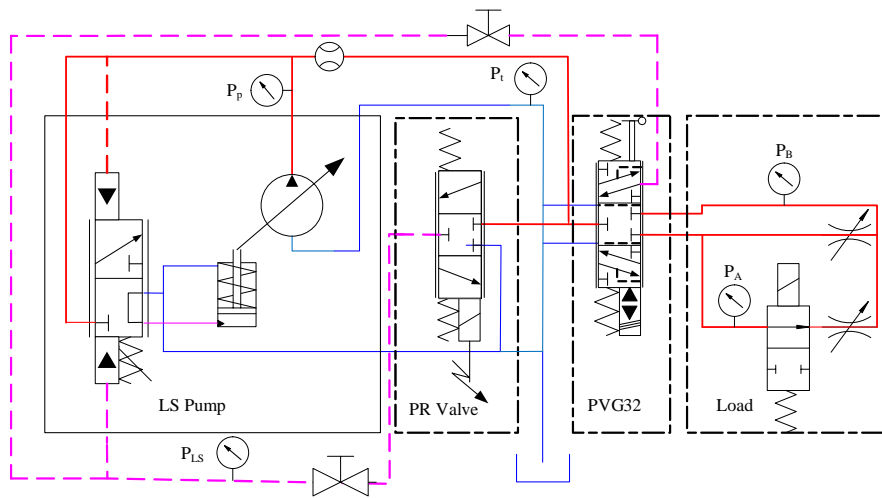


Figure 1: Diagram of the experimental set-up with indication of the various components.

The system consists of a $57[cm^3]$ Sauer-Danfoss series 45 H-frame pump, a load system consisting of a PVG 32 pressure compensated proportional valve, two variable orifices connected

in parallel and an on-off valve. The spool valve (Pressure Regulating-valve) used is a 3/3-NC under lap valve. The PR-valve is actuated with a voice coil connected to a DC/DC inverter, by which the voice coil may be current controlled.

2.1 Pressure regulating valve

The purpose of PR-valve is to control the flow to/from the pilot line, hereby generating the hydraulic LS-pressure. The reference is a measured electrical LS pressure signal. A schematic drawing of the valve is shown in figure 2 with indication of the used notation.

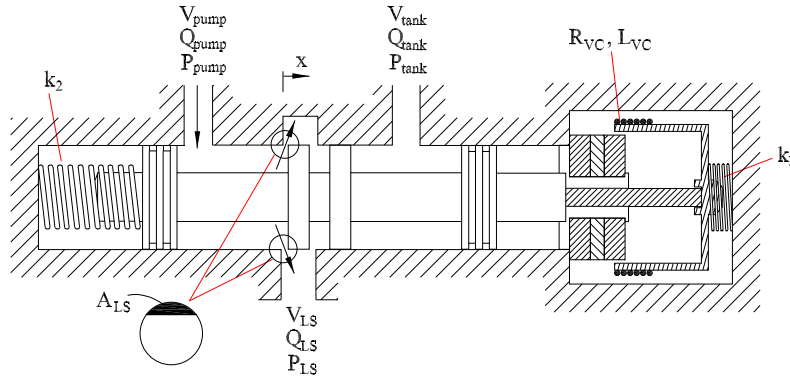


Figure 2: Model view of the spool valve with used notation.

The flow through the valve is described by the orifice equation and a laminar term describing the flow from a notch in the spool

$$Q_{LS} = \begin{cases} C_d \cdot A_{LS}(x) \cdot \sqrt{\frac{2}{\rho} \cdot (P_P - P_{LS})} - K_{lam} \cdot P_{LS} & , \quad 0 \leq x < x_l \\ C_d \cdot A_{LS}(x) \cdot \sqrt{\frac{2}{\rho} \cdot (P_P - P_{LS})} & , \quad x \geq x_l \\ -C_d \cdot A_{LS}(x) \cdot \sqrt{\frac{2}{\rho} \cdot (P_{LS} - P_T)} & , \quad x < 0 \end{cases} \quad (1)$$

Where x_l is the length of a notch made in the spool, and K_{lam} is a laminar flow coefficient. To determine the spool dynamics and hence position, the free-body diagram shown in figure 3 is considered.

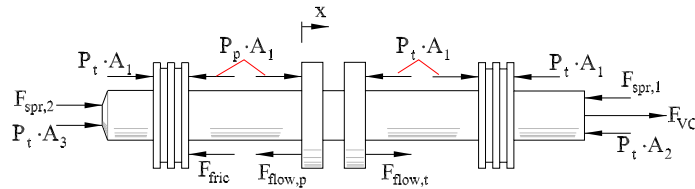


Figure 3: Forces acting on the spool.

From the figure it may be seen that the spool is pressure balanced. The force equilibrium for the spool may therefore be written as:

$$m_{spool} \cdot \ddot{x} = F_{VC} + F_{spr} - F_{flow,p} + F_{flow,t} - F_{fric} \quad (2)$$

where m_{spool} is the movable mass (including voice coil etc.). $F_{spr} = x_{spool} \cdot (k_1 - k_2) + F_{spr,0}$ is the spring force, $F_{flow,p}$ and $F_{flow,t}$ are the flow forces for the pump side and tank side valve openings respectively and F_{fric} is the friction force. F_{VC} is the voice coil force, which is proportional to the current in the voice coil, which again may be found from the voltage equation, i.e.

$$u_{VC} = R_{VC} i_{VC} + L_{VC} \frac{di}{dt} + K_m \dot{x} \quad (3)$$

$$F_{VC} = K_m \cdot i_{VC} \quad (4)$$

where $K_m \dot{x}$ is the back emf and K_m is the voice coil force constant.

The friction force is modelled as a combination of stiction, Coulomb and viscous friction as

$$F_{fric} = \begin{cases} F_{VC} + F_{spr} - F_{flow,p} + F_{flow,t} & , \dot{x} = 0 \wedge F_{VC} + F_{spr} - F_{flow,p} + F_{flow,t} < F_s \\ F_c \cdot \text{sign}(\dot{x}) + B \cdot \dot{x} & , |\dot{x}| > 0 \end{cases} \quad (5)$$

Where F_c is the Coulomb friction, F_s the stiction force and B the viscous friction coefficient. Finally, the flow forces are modelled as purely stationary flow forces, i.e. for the pump side

$$F_{flow,p} = 2 \cdot C_d \cdot A_{LS}(s) \cdot (P_P - P_{LS}) \cdot \cos(\theta) \quad (6)$$

and similarly for the tank side opening.

2.2 Pump, Volumes and Load Models

The other components in the system considered include the pump, volumes (hoses) and the load model. Considering first the different volumes in the system, these are generally described using the continuity equation, which for the LS-hose volume yields:

$$\frac{V_{LS}}{\beta} \frac{dp}{dt} + \frac{dV_{LS}}{dt} = Q_{in} - Q_{out} \quad (7)$$

With Q_{in} and Q_{out} being the flows in and out of the volume and β the effective oil bulk modulus. The latter is modelled as being pressure dependent as described in e.g. [9]. The load consists of the two variable orifices, which are simply described by the orifice equation, whereas the on-off valve is simply modelled as a switch. The load is here only used to generate a load pressure for a given pump flow. As described earlier the pump is a Sauer-Danfoss series 45 H-frame pump. The model is quite comprehensive and is presented in [10].

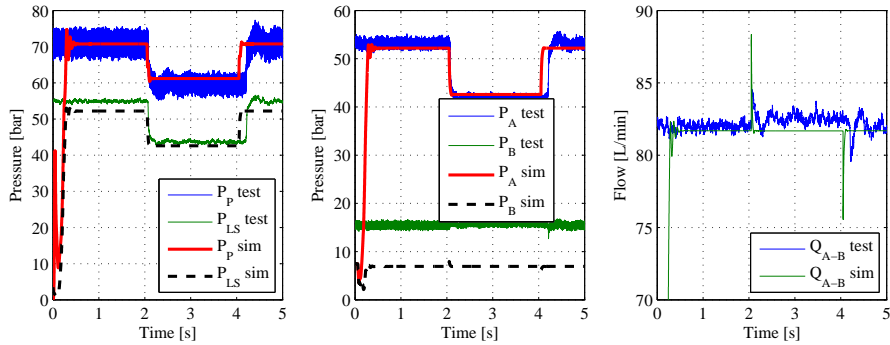


Figure 4: System response when applying load pressure steps.

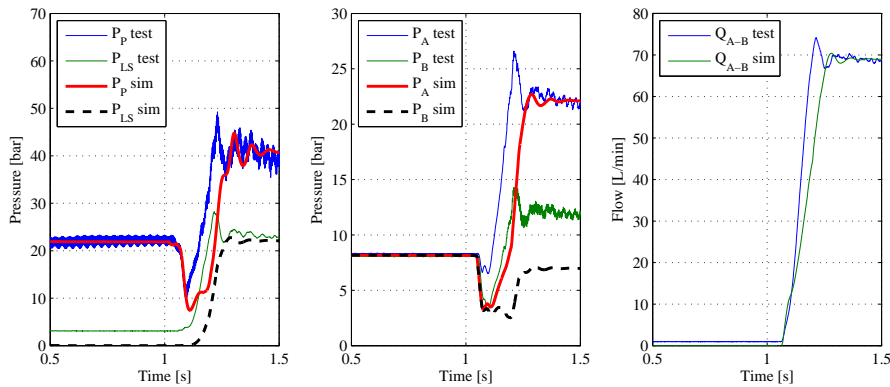


Figure 5: Step at the flow from 0 to 70 [L/min] and constant load.

2.3 Verification of Model

To verify the non-linear model and obtain performance data for the benchmark system, results from the simulation model are compared to experimental data for three different operating situations. The results of these tests are shown in figures 4- 6 on the following page below.

From the different results it may be seen that there generally is a good agreement between the measured and the simulated data. There are minor deviations, which are due to simplifications in the modelling, but the model shows the correct tendencies capturing the dominant dynamics. The model is therefore considered valid as basis for the controller design and testing.

3 LINEARISED MODEL

Based on the above described non-linear model a linearized model may be derived. This is done under the approximation that bulk modulus, discharge angle and discharge coefficients are constant. Linearising and Laplace transforming then yield the following system

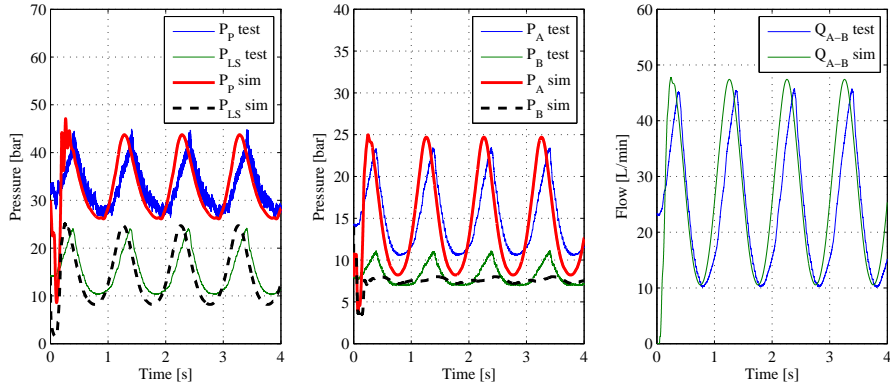


Figure 6: Sinusoidal input with frequency of 1 [Hz].

equations:

$$m_{spool} \cdot s^2 \cdot x = K_f \cdot i_{VC} - K_{spr,fq} \cdot x + K_{fqpt} \cdot P_{LS} + K_{fqpp} \cdot P_p - B \cdot s \cdot x \quad (8)$$

$$q_{LS} = K_{qpt} \cdot x - (K_{qpt} + K_{lam}) \cdot p_{LS} + K_{qp} \cdot p_p \quad (9)$$

$$p_{LS} = \frac{\beta}{s \cdot V_{LS}} \cdot q_{LS} \quad (10)$$

$$u_{VC} = R_{VC} \cdot i_{VC} + L_{VC} \cdot s \cdot i_{VC} + K_{g,VC} \cdot s \cdot x \quad (11)$$

The first expression here describe the linearised spool force equilibrium, the second the flow to the LS-hose, the third the pressure build up in the LS-hose and the fourth the voice coil dynamics. Combining these equations in block diagram form, the block diagram shown in figure 7 may be obtained.

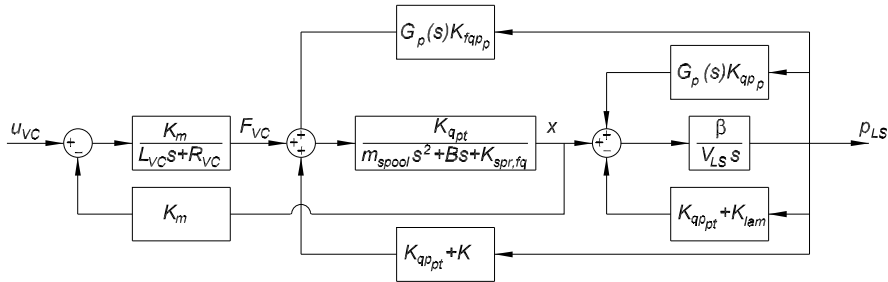


Figure 7: Block diagram relating valve voltage input ($u_{p,LS}$) to pressure in the LS-line (p_{LS}).

In the block diagram the term, $G_p(s)$, represents the pump and pump volume dynamics. As a rough approximation this is modelled by a first order filter:

$$G_p(s) = \frac{p_p}{p_{LS}} = \frac{1}{\tau_p \cdot s + 1} \quad (12)$$

To simplify the following analysis, the system may be considered in two different situations, where in the first the valve opens for connection between pump volume and the LS-hose (pump side connection), whereas in the second situation the valve opens to tank. As the system is current controlled the analysis is further simplified. For the case where the valve opens to the pump side the transfer function for the system may then be found to be

$$G_{LS,p}(s) = \frac{p_{LS}}{i_{VC}} = \frac{\beta K_{q,pt} K_f (\tau_p s + 1)}{G_d(s) (m_{spool} s^2 + B s + K_{spr,fq}) - (\tau_p s + 1) \beta K_{qp,t} K_{fq,pt} - \beta K_{q,pt} k_{fq,p}} \quad (13)$$

where $G_d(s) = ((V_{LS} s + \beta K_{qp,t} + \beta K_{leak}) (\tau_p s + 1) - \beta K_{qp,p})$. For the tank side connection case the system transfer function reduces to:

$$G_{LS,t}(s) = \frac{\beta K_{q,pt} K_f}{(V_{LS} s + \beta K_{qp,t} + \beta K_{leak}) (m_{spool} s^2 + B s + K_{spr,fq}) - \beta K_{q,pt} K_{fq,pt}} \quad (14)$$

4 STABILITY AND SENSITIVITY ANALYSIS

In order to determine a control strategy for the system, it must be determined under which operating conditions the system is likely to become unstable. The main influence is due to the pressure drop over the spool valve, Δp , the spool position, x , and the pump time constant, τ_p (dependent on pump volume and pump type). In order to investigate this influence the poles variations for varying operating conditions are investigated by looking at pole variations.

4.1 Pump side

The open loop pump side transfer function given in eq. (13) has four poles and one zero. The zero originates from the pump dynamics, always being in the left half plane and hence being of no interest at this point. Therefore, only the movement of the four poles is considered. The results of varying the pressure drop over the spool and the spool travel are shown in the figures (8) and (9).

From these results it may be seen that increasing the pressure drop¹ over the spool does not have a major influence on the dominating poles, but does mean that the damping is decreased. Increasing the spool position does however have major influence on the dominant dynamics, where large spool movements may actually lead to an unstable system in combination with the highest pressure drops. In reality it is, however, very unlikely that these worst case operating points may ever be reached, as a full spool travel in combination with the highest possible pressure drop of 18 [bar] will yield unrealistic operation conditions. From simulations with the non-linear model described in section 2, it has been found that realistic flow requirements are around 1.35[l/min]. Plotting the pole locations for varying pressure drop and spool displacement yields the plot shown in figure 10 when ensuring a flow of 1.35[l/min]. Based on this plot, the worst case working point for the pump side is therefore found to be for a pressure drop of $\Delta p = 18[Bar]$ and a spool displacement $x = 0.277[mm]$.

¹The pressure drop cannot exceed the pressure margin of the pump, which is 18[bar].

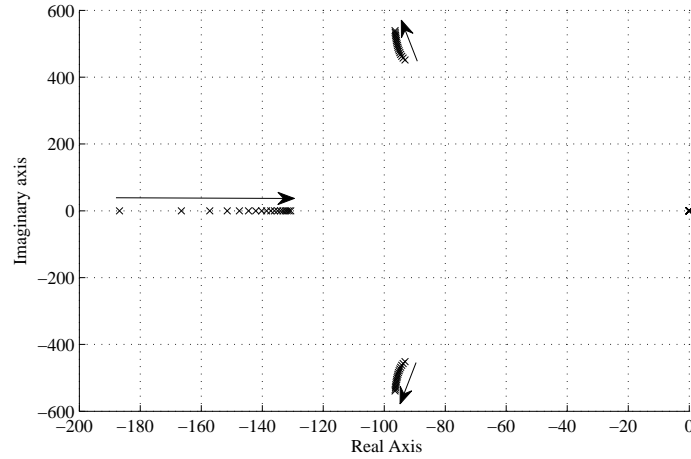


Figure 8: Pole movement for pressure drop $\Delta p = p_p - p_{LS} \in [1 - 18] [bar]$.

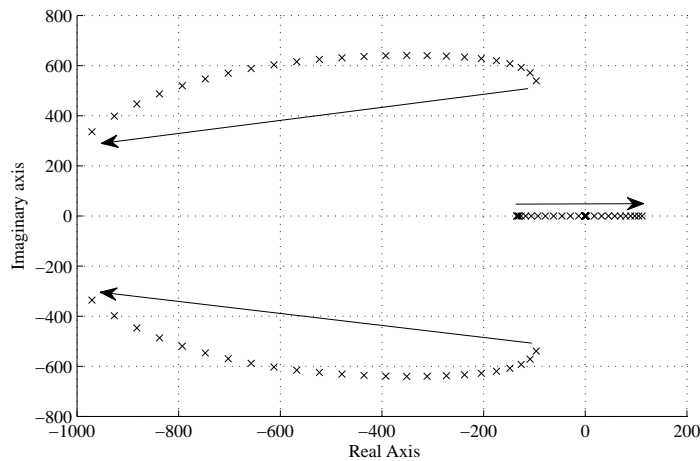


Figure 9: Pole movement at $\Delta p = p_p - p_{LS} = 18[bar]$ and spool position from $x \in [0.01 - 2.5] [mm]$.

4.2 Tank side

For the tank side the transfer function defined in eq. (14) has three poles and no zeros. As oppose to the pump side, the pump and pump volume dynamics is not influencing the tank side dynamics and hence the linearisation point will only be dependent on the pressure drop over spool ($\Delta p = p_{LS} - p_T$) and the spool position. The pressure drop over the spool is, on the other hand, only bounded by the maximum pressure in the system, why the pressure drop in opening situation may be very large. The stability and damping of the system for varying

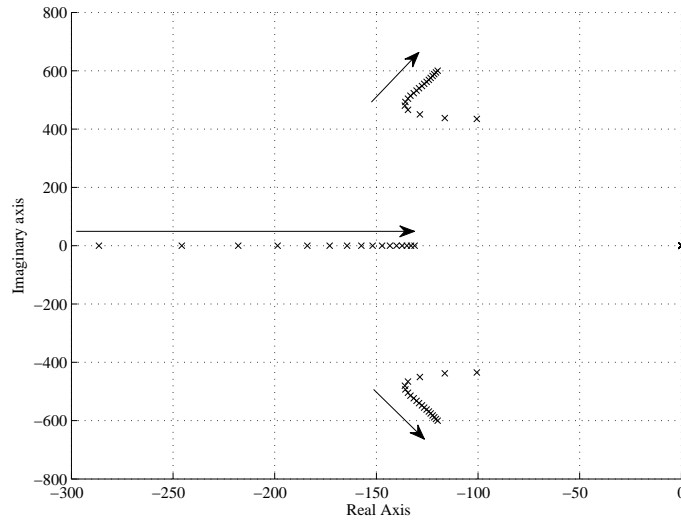


Figure 10: Pole movement at 1.35 [l/min] for rising pressure and hence decreasing spool displacement.

pressure drop and spool opening may be seen in figures 11 and 12.

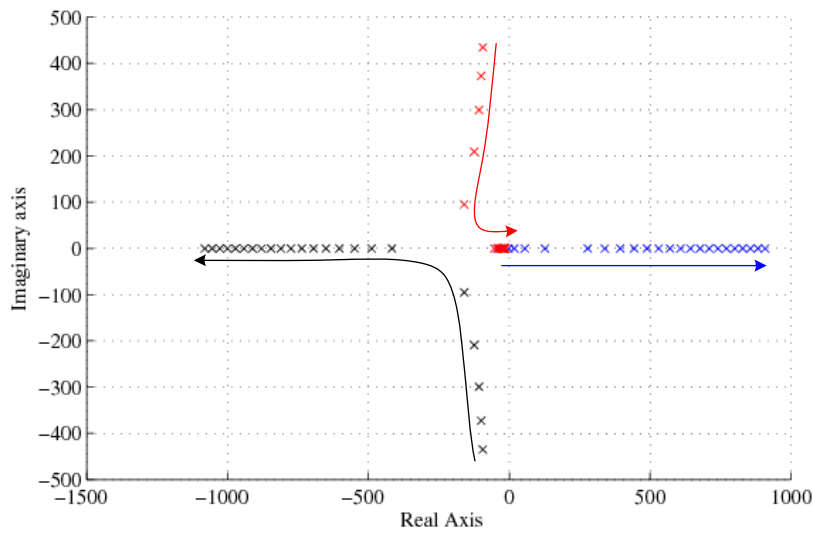


Figure 11: Pole movement for pressure drop 1-250 [bar].

For the higher pressure drops ($> 30[bar]$) the system has one of the poles in the right half plane and is therefore unstable. As for the pump side the worst case operating point is for the

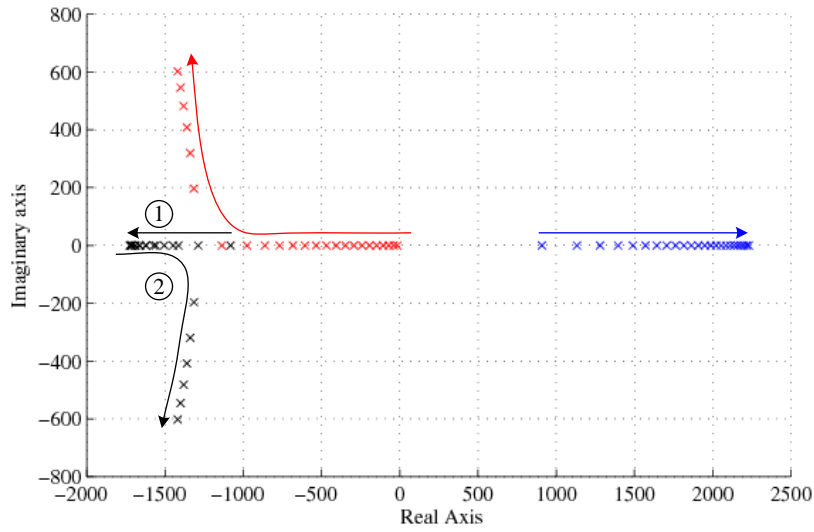


Figure 12: Pole movement at 250 [bar] and spool position from 0.01-2.5 [mm].

highest possible pressure drop and the flow requirement of 1.35[l/min]. This correspond to $\Delta p = 250[\text{bar}]$ and $x = 0.114[\text{mm}]$.

4.3 Sensitivity to varying LS-Hose Volume

The LS-hose volume directly influences the (open loop) system gain, i.e. the larger the volume, the lower the system gain. To illustrate this influence on the stability, the pole location as a function of the LS-hose volume is shown in figure 13 for the pump side case and figure 14 for the tank side case. The variations are made for $V_{LS} \in [20[\text{ml}], 320[\text{ml}]]$.

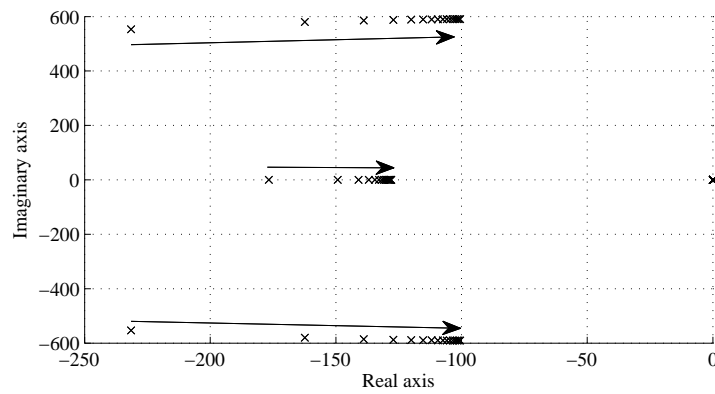


Figure 13: Open-loop poles location on pump side when considering LS-hose volume variations.

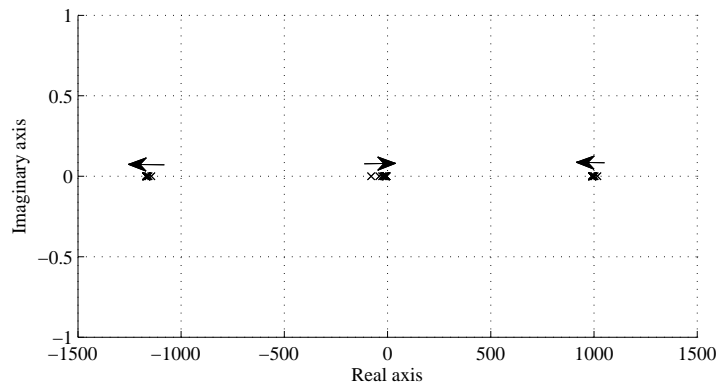


Figure 14: Open-loop poles location on tank side when considering LS-hose volume variations.

As expected the dominant system eigen frequency is lowered and the damping increased for the pump side when the volume is increased, and hence the system becomes slower. For the tank side the variation of the LS-volume is of minor influence.

5 CONTROLLER DESIGN

The basic demands of the system are that the performance must be comparable to that of the benchmark system, and that the control system is robust to changes in the system layout, i.e. hose volumes and pump type. Basically, as the system structure changes dependent on the spool position (i.e. open between pump side and LS-hose or between LS-hose and tank side), two controllers should be considered - one for each opening situation. Utilising this type of control structure, however, requires correct handling of the transition situation, where the spool crosses the zero position and the system structure changes. The situation is further complicated by the fact that the tank side dynamics is very sensitive to the pressure in the LS hose, and even becomes unstable for a pressure drop above approximately 30 bars, as shown in the previous sections. One way to overcome the switching problems is to use a kind of pressure dividing, by making a notch in the spool, allowing flow to pass from the LS hose to tank. By proper design of the area characteristic of the notch, crossing the zero position will only take place when the LS pressure is small (less than approximately 30 bars), i.e. we need to dump a relatively large amount of flow. In this situation the tank side dynamics will be stable and we can handle both situations with the same controller. Also, by allowing the spool to cross the zero position will decrease the loss inevitable arising from the "leakage" flow.

The system dynamics can now in both cases approximately be described by a relatively well damped third order system. However, the flow from the notch will change the system type from being a type 1 to being a type 0 system. Based on these considerations a standard PI-controller is utilised.

$$G_{cp}(s) = 0.69 \cdot \left(1 + \frac{1}{1.5 \cdot s} \right) \quad (15)$$

The open-loop bode plot of the system with applied PI-controller is shown in figure 15.

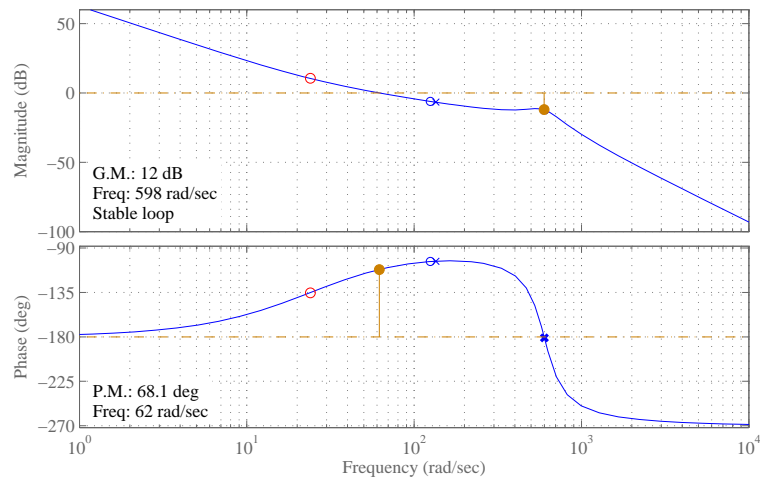


Figure 15: Open-loop bode plot of the pump side with the PI-controller. The circles and crosses representing respectively the zeros and the poles of the system, with the the first circle (red) resulting from the zero added by the PI-controller.

Based on the above analysis the designed controller has been implemented and tested experimentally. The results are shown in figures 16-18.

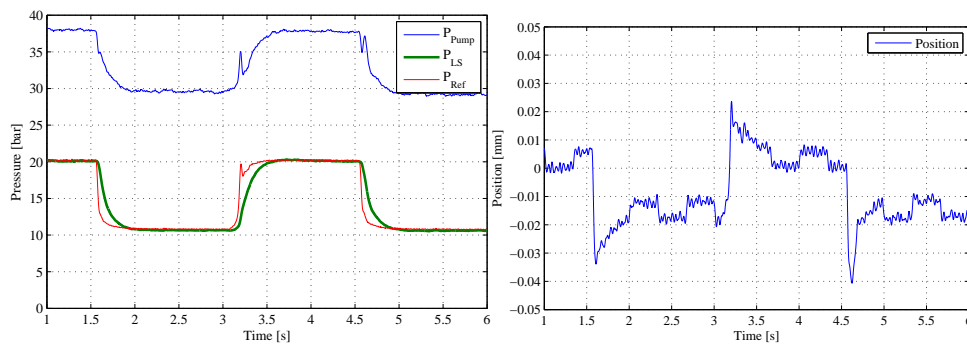


Figure 16: Measured pressure and spool position when operating at low pressures and applying pressure steps.

From the results it may be seen that the system is operating as expected. For small pressure steps the system is continuously operating with a positive spool position, as seen in Fig. 17, meaning that the system is continuously controlling the leakage flow to tank. For the larger

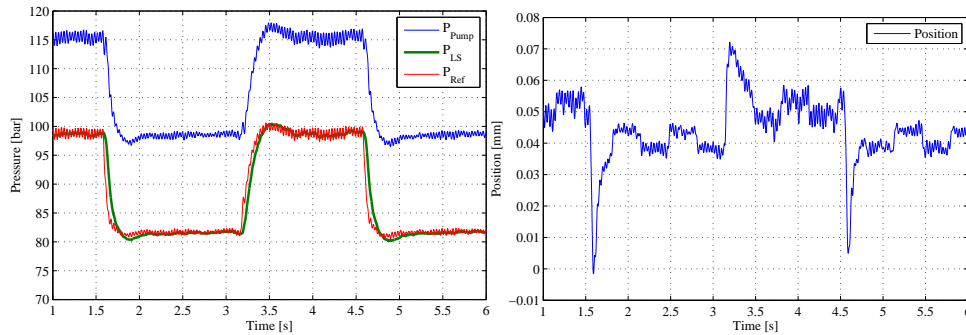


Figure 17: Measured pressure and spool position when operating at high load pressure and applying minor pressure steps.

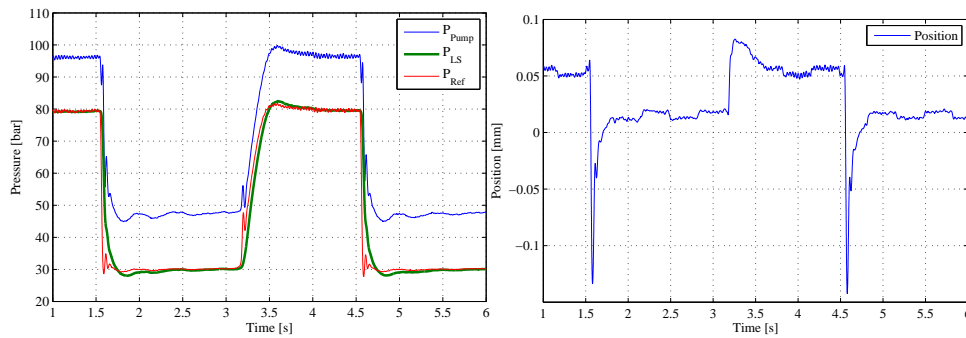


Figure 18: Measured data for high load pressure and large pressure steps.

downwards pressure steps and when operating at low system pressure (Fig. 18 and 16 respectively), the leakage flow is however not large enough, to wash out the pump sufficiently fast, why the valve switches over and operates with a negative spool position. In this case the pressure drop over the spool have, however been lowered (due to the initial leakage flow), to a level where the system is not unstable, cf. the above analysis.

6 CONCLUSION

The focus of this paper has been on generating a hydraulic (LS) pilot pressure based on an electric reference for use in systems without hydraulic feedback of the load pressure. This was done using a small spool valve, where a model of the valve and the considered system was first presented. A linear analysis of the system yielded the worst case operating conditions of the system, and based on this analysis an approach using a controlled leakage flow was utilised, hereby enabling the system to be operated with a simple PI-controller and still be stable and robust towards transitions between pump and tank side operation. Finally experimental results were presented showing the validity of the approach.

References

- [1] H.H. Harms. Hydraulic fluid technology: Current problems and future challenges. In *International Exposition for Power Transmission and Technical Conference*, Apr. 2000.
- [2] A. Langen. *Experimentelle und analytische Untersuchungen an vergesteuerten hydraulisch-mechanischen und elektro-hydraulischen pumpeuregulungen*. PhD thesis, Rheinisch-Westfälischen Technischen Hochschule Aachen, 1986.
- [3] H. Esders. *Elektrohydraulisches Load Sensing für mobile Anwendungen*. PhD thesis, Technischen Universität Carolo Wilhelmina zu Braunschweig, 1995.
- [4] B. Lantto. *On Fluid Power Control - with Special Reference to Load-Sensing Systems and Sliding Mode Control*. PhD thesis, Linköping, 1994.
- [5] G. Tewes and H.H. Harms. Fuzzy control for an electrohydraulic load-sensing system. In *Fluid Power Systems, Ninth Bath International Fluid Power Workshop*, Sep. 1996.
- [6] B. Zähe. *Energiesparende Schaltungen hydraulischer Antrieb mit veränderlichem Versorgungsdruck und ihre Regelung*. PhD thesis, Rheinisch-Westfälischen Technischen Hochschule Aachen, 1993.
- [7] W. Backé and B. Zähe. Electrohydraulic load-sensing. *SAE Technical Paper Series*, 1991.
- [8] P. Krus, T. Persson, and J.-O. Palmberg. Complementary control of pressure control pumps. In *Proceedings of the IASTED International Symposium, MIC'88*, 1988.
- [9] B. Nielsen, H.C. Pedersen, T.O. Andersen, and M.R. Hansen. Modelling and simulation of mobile hydraulic crane with telescopic arm. In J.S. Stecki, editor, *1st International Conference on Computational Methods in Fluid Power Technology*, pages 145–154, Melbourne, Australia, Nov. 2003.
- [10] H.C. Pedersen, T.O. Andersen, and M.R. Hansen. Designing an electro-hydraulic control module for an open-circuit variable displacement pump. In *Proc. of The Ninth Scandinavian International Conference on Fluid Power, SICFP05*, Linköping, Sweden, June 2005. SICFP05.